Thermochimica Acta 520 (2011) 84–92

Contents lists available at ScienceDirect

Thermochimica Acta

journal homepage: www.elsevier.com/locate/tca

Effect of cashew nut shell liquid on gelation, cure kinetics, and thermomechanical properties of benzoxazine resin

Pornnapa Kasemsiri[a], Salim Hiziroglu[b], Sarawut Rimdusit[a,*]

[a] Department of Chemical Engineering, Faculty of Engineering, Chulalongkorn University, Pathumwon, Bangkok 10330, Thailand
[b] Department of Natural Resource Ecology and Management, Oklahoma State University, 303-G Agricultural Hall, Stillwater, OK 74078, USA

ARTICLE INFO

Article history:
Received 23 December 2010
Received in revised form 14 March 2011
Accepted 25 March 2011
Available online 5 April 2011

Keywords:
Cashew nut shell liquid
Benzoxazine resin
Gelation
Curing kinetics
Wood composite

ABSTRACT

Effects of cashew nut shell liquid (CNSL) on properties of a bifunctional benzoxazine resin (BA-a) have been investigated. The CNSL remarkably decreases the liquefying temperature, gel time and curing temperature of the neat benzoxazine resin. The Kissinger and Ozawa methods are used to calculate the curing kinetic parameters of BA-a/CNSL systems. The activation energy values obtained from both models show fairly consistent results i.e. the activation energy values decrease with increasing the CNSL content. It was found that optimal CNSL content from solvent extraction experiment should not exceed 20 wt% to avoid the presence of unreacted CNSL in the alloy network. Properties of bamboo fiber-reinforced BA-a/CNSL alloys are also investigated in this work. The filled BA-a/CNSL at 65 wt% of bamboo fiber shows a substantial increase in storage modulus and T_g of the composites. BA-a/CNSL alloy shows great potential as high performance lignocellulosic adhesive for wood composite applications.

1. Introduction

Benzoxazine resins are new members of phenolic based adhesives. These novel types of phenolic resins have been reported to provide some outstanding characteristics such as excellent thermal properties and flame retardance, molecular design flexibility, low moisture absorption, near zero shrinkage upon polymerization, low melt viscosities, and low dielectric constant [1–4]. Therefore, polybenzoxazines are widely applied in various fields such as structural materials and adhesives especially when high strength properties are desired.

Recently, the development of the benzoxazine-based on renewable organic material has attracted significant attention. Especially, a novel cardanol-based benzoxazine monomer contains an oxazine ring in its structure. The ring can react with carbon atoms on benzene ring of cardanol which is the main component of cashew nut shell liquid (CNSL) [5]. CNSL is a blend of naturally occurring phenol-based monomer and is traditionally obtained as by-product during the process of removing the cashew kernel from the nut. The production of CNSL is nearly 25% of the total nut weight. The main producers of cashew nut are in Asia, Africa and South America. The major components of CNSL are anacardic acid, cardanol and trace of cardol and 1-methylcardol. The CNSL has various applications in different industries such as friction linings, paints and varnishes, laminating resins, rubber compounding resin, urethane based polymer, surfactant, epoxy resin, modifier agent of phenol–formaldehyde resin for plywood production and intermediate for chemical industries. It also has potential and opportunities for development of other tailor-made polymers. This makes CNSL and their components become important for new value-added materials with possible industrial uses [6–8]. Consequently, CNSL is an excellent candidate material to modify properties of benzoxazine resin and a potential of reducing a material cost.

Currently there is no information on properties of BA-a/CNSL alloys. Therefore, effects of the benzoxazine resin modified with cashew nut shell liquid oil on the resulting processing ability and kinetic parameters of the curing process will be investigated in this research. Furthermore, the thermal properties and the adhesion performance of these alloys in wood composite will also be examined.

2. Experimental

2.1. Materials

Benzoxazine resin is based on bisphenol-A, aniline and formaldehyde. The bisphenol-A (polycarbonate grade) was supplied by Thai Polycarbonate Co., Ltd. (TPCC). Para-formaldehyde (AR grade) and aniline (AR grade) were purchased from Merck Ltd. and Panreac Quimica S.A. The CNSL was contributed by Maboonkrong Sirichai 25 Ltd. Bamboo fiber (*Dendrocalamus asper*) was supplied by Forest Products Division, Royal Forest Department, Thailand.

* Corresponding author. Tel.: +66 2 218 6862; fax: +66 2 218 6877.
E-mail address: sarawut.r@chula.ac.th (S. Rimdusit).

0040-6031/$ – see front matter © 2011 Elsevier B.V. All rights reserved.
doi:10.1016/j.tca.2011.03.020

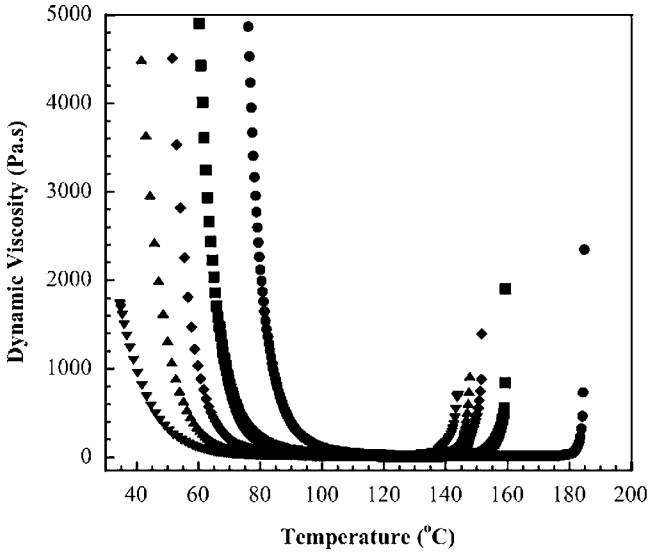

Fig. 1. Viscosity of BA-a/CNSL resin at various compositions: (●) BA-a/CNSL 100/0, (■) BA-a/CNSL 90/10, (♦) BA-a/CNSL 80/20, (▲) BA-a/CNSL 70/30 and (▼) BA-a/CNSL 60/40.

2.2. Preparation of benzoxazine–cashew nut oil matrix

Benzoxazine monomer used was synthesized from bisphenol A, aniline and formaldehyde at a molecular ratio of 1:2:4. The monomer synthesis was based on the patented solventless synthesis technique [9]. The reactants were physically mixed and heated to their melting point temperature thereafter maintained at a temperature sufficient to complete the interaction of the reactants to produce the benzoxazine monomer [10]. The BA-a blended with CNSL was used as a composite matrix and was prepared at temperature of 80 °C.

2.3. Preparation of wood-BA-a/CSNL alloy composites

Bamboo fiber was dried at temperature of 100 °C for 24 h to get a constant weight. A fixed bamboo fiber content of 65 wt% was compounded with BA-a/CSNL mixture in an aluminum container at 80 °C for at least 30 min in order to ensure fiber wet-out by the resin. Due to the relatively low viscosity of the matrix at 80 °C, the fiber can be impregnated by manual mixing following the method in Refs. [32,33]. The viscosity of all matrices was illustrated in Fig. 1. The compound was placed in a preheated 60 mm × 25 mm × 3 mm stainless steel mold and compressed in a hydraulic press using a pressure of 15 MPa and at temperature of 110 °C for 0.5 h and 170 °C for 3.5 h. The cured specimens were left to cool down at room temperature in an open mold before testing.

2.4. Evaluation of chemorheological properties

Chemorheological properties of each alloy were examined using a rheometer (Haake Rheo Stress 600, Thermo Electron Cooperation) equipped with 35 mm in diameter parallel plate geometry. The measuring gap was set at 0.5 mm. The experiment was performed under an oscillatory shear mode at 1 rad s^{-1}. The testing temperature program was ramped from room temperature at a heating rate of 2 °C min^{-1} to a temperature beyond the gel point of each resin and the dynamic viscosity was recorded.

2.5. Evaluation of curing reaction and kinetic parameters of BA-a/CSNL matrices

The curing behavior and kinetic parameters were measured by a differential scanning calorimeter (DSC) model 2910 from TA Instrument. The heating rates were 1, 3, 5 and 10 °C min^{-1} from 30 to 300 °C under nitrogen gas purging.

2.6. Evaluation of curing behavior of BA-a/CNSL blends

Fourier transform infrared spectra of all samples under various curing conditions were acquired by using a Spectrum GX FT-IR spectrometer from Perkin Elmer. All spectra were taken as a function of time with 64 scans at a resolution of 4 cm^{-1} and a spectral range of 4000–650 cm^{-1}. The powder sample was mixed with KBr powder. The mixed powder was pressed into pellet before measurement.

2.7. Mechanical properties analysis

The dynamic mechanical analyzer (DMA) model DMA 242 from NETZSCH was used to investigate the dynamic mechanical properties and relaxation behaviors of BA-a/CNSL polymer alloys. The dimension of specimens was 10 mm × 50 mm × 2 mm. The test was performed in a three-point-bending mode. In a temperature sweep experiment, a frequency of 1 Hz and a strain value of 0.1% were applied. The temperature was scanned from room temperature to T_g of each specimen with a heating rate of 2 °C min^{-1} under nitrogen atmosphere.

The flexural modulus and flexural strength of the wood composite specimens were determined according ASTM D790 employing a Universal Testing Machine, Instron, Model 5567 equipped with a 1 kN load cell. The measurement was performed in a 3-point bending mode with a support span of 48 mm and at a crosshead speed of 1.2 mm/min. A minimum of five samples with a dimension of 25 mm × 60 mm × 3 mm was tested and the averaged values were determined.

3. Results and discussion

3.1. Chemorheological properties of BA-a/CNSL resin mixtures

The complex viscosity values of the BA-a, 90/10 BA-a/CNSL, 80/20 BA-a/CNSL, 70/30 BA-a/CNSL and 60/40 BA-a/CNSL as a function of temperature are illustrated in Fig. 1. During heating, these uncured monomers became softened and viscosity rapidly decreased as temperature approached their softening points. The next stage was the lowest viscosity range of the resin mixtures as all compositions became liquid. This stage provided a processing window for the compounding process of each alloy. At the final stage, the binary mixture underwent crosslinking reactions past their gel points resulting in a sharp increase in their viscosities.

As seen from Fig. 1, the temperature of resin mixture was ramped from 40 °C up to beyond the gel point of each sample using a heating rate of 2 °C min^{-1} and a dynamic viscosity was recorded. On the left hand side of Fig. 1, the liquefying temperature of the binary mixture was indicated by the lowest temperature that the viscosity rapidly approached its minimum value. For consistency, the temperature at the viscosity value of 1000 Pa s was used to determine liquefying temperature of each resin [11]. The liquefying temperature significantly decreased with increasing amount of cashew nut shell liquid oil fraction i.e. 83 °C (BA-a), 68 °C (90/10 BA-a/CNSL), 59 °C (80/20 BA-a/CNSL), 50 °C (70/30 BA-a/CNSL) and 39 °C (60/40 BA-a/CNSL). This may be due to the fact that the CNSL is liquid while benzoxazine resin is solid at room temperature. Therefore addition of liquid (CNSL) in the solid (BA-a resin) resulted in

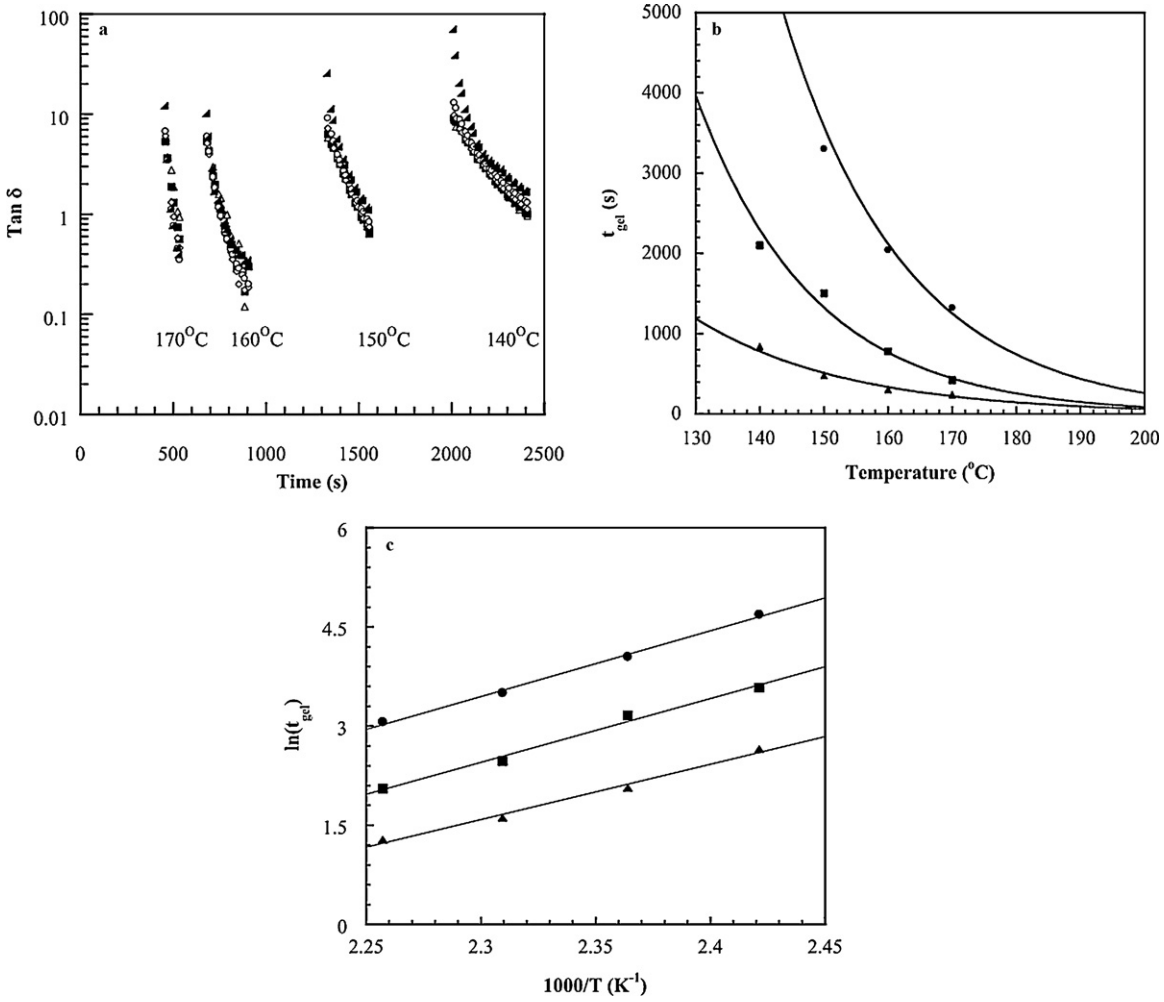

Fig. 2. (a) Effect of gel temperature on the gel time of BA-a mixed with CNSL at composition 90:10 (●) 1.6 Hz, (□) 2.8 Hz, (♦) 5.0 Hz, (△) 9.0 Hz and (▼) 15.9 Hz. (b) Gelation behavior of BA-a/CNSL revealing the gel time as a function of gel temperature at compositions: (●) BA-a/CNSL 100/0, (■) BA-a/CNSL 90/10 and (▲) BA-a/CNSL 70/30. (c) The Arrhenius plot of the gelation behavior of BA-a/CNSL at compositions: (●) BA-a/CNSL 100/0, (■) BA-a/CNSL 90/10 and (▲) BA-a/CNSL 70/30.

softer material at room temperature with lower liquefying point. The lowest viscosity at room temperature was observed in a 40 wt% CNSL system. In practice, lowering the resin liquefying temperature obviously enables the use of lower processing temperature for a compounding process, which is desirable in various applications.

On the right hand side of Fig. 1, gel temperature of each resin mixture can be evaluated. The temperature at which viscosity was rapidly raised above 1000 Pa s was used to indicate gel temperature of each resin [11]. The gel temperatures tended to decrease with increasing the CNSL content i.e. the gel temperatures of BA-a, 90/10 BA-a/CNSL, 80/20 BA-a/CNSL, 70/30 BA-a/CNSL and 60/40 BA-a/CNSL were observed to be 184, 159, 152, 147 and 143 °C, respectively. This result implied that CNSL can be not only a reactive diluent for benzoxazine resin but also a good initiator to lower the curing temperature or gel point of the benzoxazine resin.

3.2. Evaluation of activation energy of BA-a/CNSL resin mixtures

Some of the important aspects of thermosetting polymer include their gelation behavior, kinetic of gelation and the gel time. Sol–gel or gel point is one critical phenomenon that is crucial for the material processing. The gel points of samples can be accurately determined by dynamic rheological measurements which are sensitive to degree of crosslinking. In principle, elastic modulus and viscous modulus present the same power-law variation with respect to the frequency of oscillation at a gel point [12]. The corresponding expressions describing the dynamic moduli at the gel point were as follow:

$$\tan\delta = \frac{G''}{G'} = \tan\left(\frac{n\pi}{2}\right) \quad (1)$$

where G' is storage modulus, G'' is loss modulus and n is the relaxation exponent which is network specific. The above expression suggests frequency independent nature of tan δ at gel point. Experimentally, this is the point where tan δ curves of various frequencies crossover each other.

Fig. 2(a) shows the gel point of BA-a/CNSL at 90/10 mass ratio which was cured isothermally at 140, 150, 160 and 170 °C and at different frequencies i.e. 1.6, 2.8, 5, 9 and 15.6 Hz as a function of time (s). From the plot, the points that tan δ is frequency independent were at time equal 35 min (140 °C), 25 min (150 °C), 13 min (160 °C) and 7 min (170 °C) corresponding to the gel time at each temperature. The gel times of the resin mixtures expectedly decreased with increasing temperature. Gel times of other BA-a/CNSL systems at different temperatures were also obtained from the tan δ plots similar to the result in Fig. 2(a). Fig. 2(b) illustrates a relationship between gel time and temperature of BA-a/CNSL systems at varied compositions. All resin mixtures exhibited an exponential decay behavior of the gel time with increasing temperature. This could be due to the fact that raising the processing temperature increased the rate of crosslinking of BA-a/CNSL systems. As a result, the higher

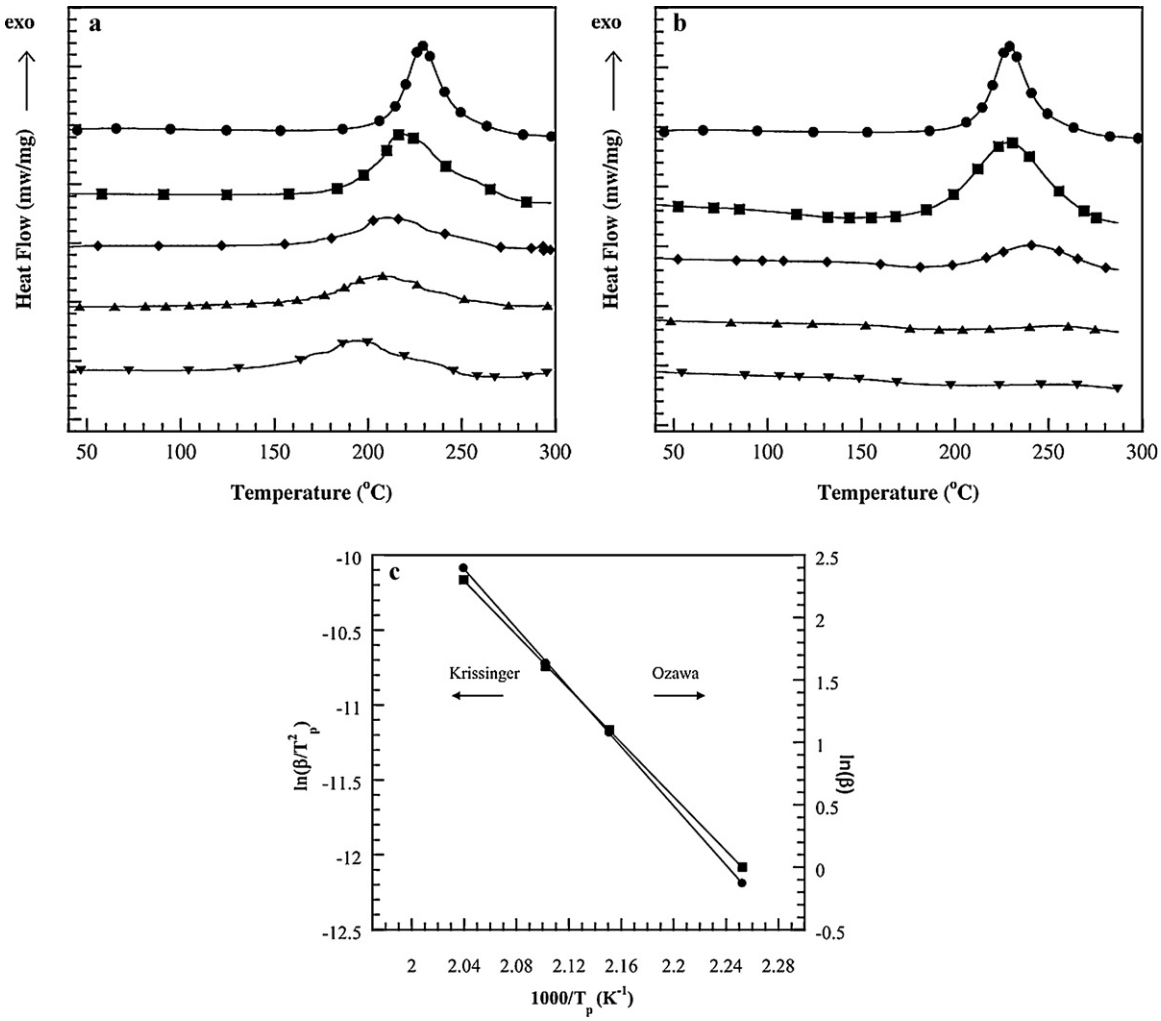

Fig. 3. (a) DSC thermograms of BA-a/CNSL resin at various compositions: (●) BA-a/CNSL 100/0, (■) BA-a/CNSL 90/10, (♦) BA-a/CNSL 80/20, (▲) BA-a/CNSL 70/30 and (▼) BA-a/CNSL 60/40. (b) DSC thermograms of BA-a at various curing conditions: (●) uncured, (■) 160 °C/1 h, (♦) 180 °C/1 h, (▲) 200 °C/1 h and (▼) 200 °C/2 h. (c) (●) Kissinger method and (■) Ozawa method plots for averaged activation energy determination of 90/10 BA-a/CNSL.

curing temperature, the faster the resin systems can reach their gel point. Additionally, from the figure, the gel time tended to decrease with increasing the CNSL content comparing at the same temperature. For instance, at 140 °C the gel time BA-a = 108 min, BA-a/CNSL 90/10 = 35 min and BA-a/CNSL 70/30 = 14 min. This result also indicated that the curing conversion of the BA-a/CNSL was raised with increasing CNSL content.

According to Winter and Chambon, $\tan\delta$ is independent of frequencies at the gel point of the polymer. The frequency independence of the loss tangent in the vicinity of the gel point has been widely used to determine the gel time (t_{gel}) in either chemical or physical gels. Additionally, activation energy of gelation process can be evaluated and calculated from the gel times at different isothermal temperatures using Arrhenius model following Eq. (2) or (3)

$$t_{gel} = A \exp\left(\frac{\Delta E}{RT}\right) \quad (2)$$

or

$$\ln(t_{gel}) = \ln A + \left(\frac{\Delta E}{RT}\right) \quad (3)$$

where t_{gel} is gel time, A is a pre-exponential factor, E is activation energy (kJ mol^{-1}) and T is temperature (K).

Fig. 2(c) displays the Arrhenius plot revealing the effect of the reactive CNSL on the gel time of BA-a resin. The activation energy calculated from the slopes of the curves was 84 kJ mol^{-1} (BA-a), 80 kJ mol^{-1} (90/10 BA-a/CNSL) and 71 kJ mol^{-1} (70/30 BA-a/CNSL). These activation energy values decreased with increasing amount of the CNSL. Moreover, the different y-intercepts at various CNSL content in Fig. 2(c) were also related to the initial temperature that material started the gelation process. The lowest y-incept value was found in 70/30 BA-a/CNSL system while the neat BA-a provided the highest value. This result implied that the presence of 30 wt% CNSL in BA-a required lower starting temperature for the gelation process than 90/10 BA-a/CNSL or neat BA-a.

3.3. Curing reaction and thermal properties of BA-a/CNSL resins

The neat benzoxazine resin (BA-a) is designed to thermally polymerize via a ring-opening addition reaction so that it does not yield any by-product. The curing reaction takes place either with or without catalyst or initiator. In general, it is a well known fact that oxazine ring opening is initiated by the presence of acidic catalysts [13]. The curing exotherms of the resin mixtures at various weight ratios of BA-a and CNSL are illustrated in Fig. 3(a). The peak exotherm and enthalpy of curing of BA-a were observed at 237 °C and 277 J g^{-1}. In the case of BA-a/CNSL mixtures, the peak exotherms and enthalpy of cure values were found to be lower than those of BA-a. When the amount of CNSL in samples increased, both peak exothermic temperature and enthalpy of cure

Table 1
Kinetic parameters evaluated from Kissinger and Ozawa methods.

BA-a/CNSL sample	Methods	
	Kissinger (kJ mol^{-1})	Ozawa (kJ mol^{-1})
100/0	84	87
90/10	82	85
70/30	74	79

values decreased i.e. 216 °C and 246 J g^{-1} (90/10 BA-a/CNSL), 207 °C and 224 J g^{-1} (80/20 BA-a/CNSL), 203 °C and 219 J g^{-1} (70/30 BA-a/CNSL) and 197 °C and 194 J g^{-1} (60/40 BA-a/CNSL). This result suggested that the anacardic acid in CNSL might act as a curing accelerator which caused a shift of the exotherm of the ring-opening reaction of the benzoxazine resin to lower temperature. The lowering of exotherms in benzoxazine systems had also been observed by the addition of other acidic protons such as poly (amide acid), clay, and titania [14–16]. In addition, the decrease of cure exotherms of BA-a/CNSL alloys may be possibly due to the presence of phenolic compounds in CNSL such as cardanol, cardol and 1-methylcardol. These phenolic compounds can act as initiator for the ring opening oligomerization of benzoxazine compounds [16]. The decrease of curing temperature of BA-a/CNSL alloys has a positive effect on the utilization of these alloys as a matrix for lignocellulosic composites i.e. a relatively lower curing temperature, or lower energy consumption, can be used. Generally, the curing or melting temperatures of wood composite molding compounds should be kept below 200 °C, except for a short period of processing time, in order to achieve samples with good mechanical integrity. A higher temperature can result in the release of volatiles, discoloration, odor, and embrittlement of the wood component [17].

The fully cured condition of BA-a and BA-a/CNSL systems was determined from the neat BA-a resin, which required the highest curing temperature among the investigated resin mixtures as depicted in Fig. 3(a). The DSC thermograms of BA-a resin after undergoing different curing conditions were shown in Fig. 3(b). The degree of conversion estimated by Eq. (4) was determined to be 20% after curing at 160 °C for 1 h, 72% after curing at 180 °C for 1 h, 96% after curing at 200 °C for 1 h and 100% after curing at 200 °C for 2 h. At the final step, the disappearance of exothermic peak of reaction indicated the fully cured of sample.

$$\%\,\text{conversion} = 1 - \left[\left(\frac{H_{rxn}}{H_o}\right) \times 100\right] \quad (4)$$

where H_{rxn} is the exothermic heat of reaction of the partially cured specimens, as determined from DSC, and H_o is the exothermic heat of reaction of the uncured resin.

3.4. Curing kinetic model of BA-a/CNSL matrix

To determine the curing kinetic parameters of BA-a/CNSL, a non-isothermal method in DSC experiment was used. The methods are widely used to study dynamic kinetics of thermosetting polymers as proposed by Kissinger and Ozawa. The detail of each method was described in the literatures [18,19].

From the non-isothermal DSC result of 90/10 (BA-a/CNSL) by using this multi heating rate data according to the Kissinger and Ozawa method, a good linear relationship between the heating rate and the reversal of the exothermic peak temperature can be obtained as shown in Fig. 3(c). The activation energy can also be calculated from the slope of the plot. The average activation energy values of BA-a and BA-a/CNSL are summarized in Table 1. The average activation energy of BA-a resin was calculated to be 84-87 kJ mol^{-1}. This values fall in the same range as those in our previous report [19]. The average activation energy of BA-a/CNSL system trended to decrease with increasing amount of CNSL content in the resin mixture i.e. 82–85 kJ mol^{-1} for 90/10 (BA-a/CNSL) and 74–79 kJ mol^{-1} for 70/30 (BA-a/CNSL). The decreasing activation energy of BA-a with increasing content of acid media was also observed in polybenzoxazine-clay hybrid nanocomposite [20]. Furthermore, a decrease of activation energy upon increasing CNSL content also had similar trend as that obtained from Arrhenius model in the gelation process.

3.5. Curing behaviors of BA-a blended with CNSL

The curing behavior of BA-a blend with CNSL was monitored by FT-IR spectroscopy. Fig. 4 shows example of FT-IR spectra in case of BA-a/CNSL at a fixed mass ratio of 80/20. In Fig. 4(a), the characteristic infrared adsorption bands of CNSL were observed at 990 and 912 cm^{-1} which correspond to phenol containing the pendent chain at meta position. The bands at 1264 and 1156 cm^{-1} were assigned to the symmetric and asymmetric stretching of the bounding C=C, respectively and the peak at 1588 cm^{-1} also related to the stretching of carbon double (C=C). The characteristic bands at 1650 cm^{-1} was assigned to (C=O) of anacardic. The peaks at 2852 and 2922 cm^{-1} corresponded to asymmetric and symmetric stretching of CH_3 and the peak around 3320 cm^{-1} was characteristic of the stretching of OH [21–23]. For BA-a/CNSL, as shown in Fig. 4(b) the characteristic adsorption peak of BA-a were 940 and 1232 cm^{-1}, which were assigned to the benzoxazine mode of the benzene ring that is adjacent to oxazine ring and trisubstituted benzene of the oxazine ring, respectively. According to the polymerization mechanism reported by Dunkers and Ishida [24], the oxazine ring is opened by the breakage of a C–O bond in it. Thereby the benzoxazine molecule was transformed from a ring structure to a network structure. During this process, the tri-substituted benzene ring, the backbone of the benzoxazine ring, became tetra-substituted. The indication of the ring-opening polymerization of BA-a was observed from the decrease of the absorption at 940 and 1232 cm^{-1} and the appearance of new adsorption band at 1487 cm^{-1} which is tetra tetra-substituted as shown in Fig. 4(c). Furthermore, the other adsorption bands of carbonyl group appeared in the region of 1750–1550 cm^{-1} which is assigned to the strong interaction between BA-a polymer and carboxylic acid. Especially, the appearance of the band at 1285 cm^{-1}

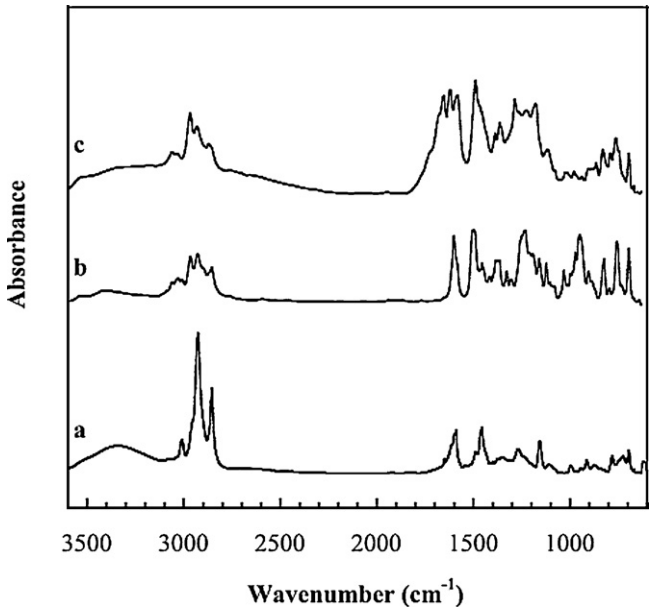

Fig. 4. IR spectra of (a) uncured CNSL, (b) uncured BA-a/CNSL 80/20 and (c) cured BA-a/CNSL 80/20 at 200 °C/2 h.

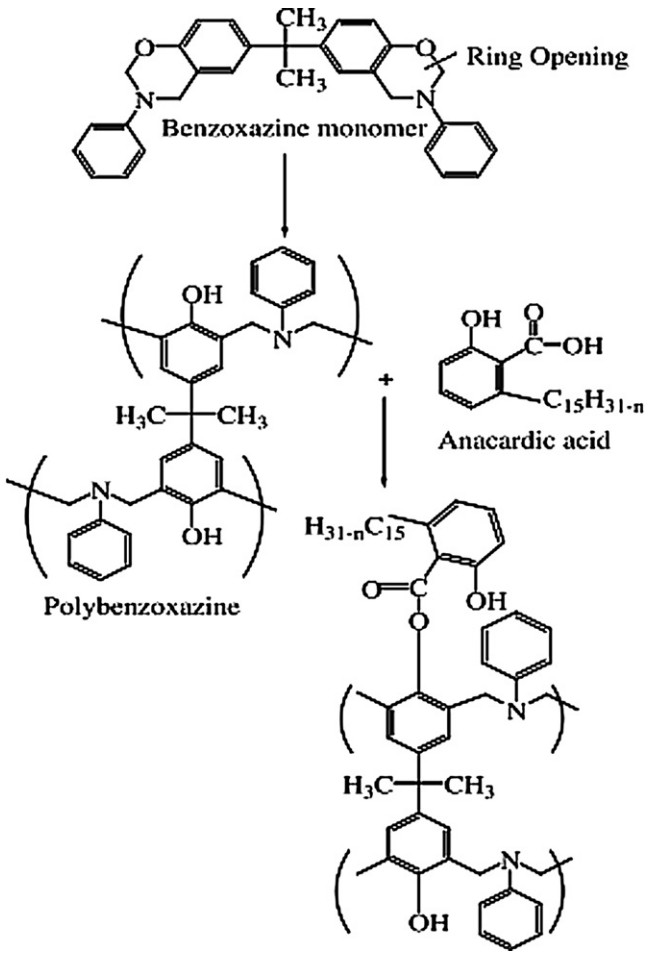

Scheme 1. A possible reaction between BA-a and CNSL.

could be assigned to the aromatic ester (Ar–COOR) that might from during curing reaction of BA-a/CNSL. This result may implied that the reaction between the phenolic (OH) of polybenzoxazine and carboxylic acid of CNSL component could occur as shown in Scheme 1. The similar reaction was also observed in the system of benzoxazine alloyed with poly (amide acid) [16].

3.6. Dynamic mechanical properties of BA-a/CNSL polymer matrix

Dynamic mechanical properties of the BA-a/CNSL alloys as a function of temperature are displayed in Fig. 5(a). The storage modulus (E') of a solid sample at room temperature provides a measure of material stiffness. The storage moduli of fully cured alloys were found to be 5.6 GPa for BA-a, 4.8 GPa for 90/10 (BA-a/CNSL), 4.7 GPa for 80/20 (BA-a/CNSL), 4.0 GPa for 70/30 (BA-a/CNSL) and 3.9 GPa for 60/40 (BA-a/CNSL). The storage moduli at room temperature of BA-a/CNSL polymers systematically decreased with increasing amount of CNSL. The decrease of storage moduli in alloys can be explained by the plasticizing effect of the CNSL on the polybenzoxazine. Though, the presence of CNSL in BA-a resulted in a more ductile polymer hybrids, the storage moduli values of BA-a/CNSL matrix were still higher than those of major unfilled thermosets used as wood composite matrices including phenolic resin (1 GPa) [25], and unsaturated polyester (8.8×10^{-3} GPa) [26].

Furthermore, the rubbery plateau modulus value in Fig. 5(a) can be used to determine crosslink density of the alloy network. In the past, some researchers have attempted to apply theory of rubber elasticity to quantify crosslink density and molecular weight between crosslinks/entanglements of network forming polymer. However, this theory is strictly applicable to lightly crosslinked materials. For highly crosslinked polymer network, the Gaussian distribution of the chain between crosslink is no longer applied and its crosslink density is more precisely estimated by the Nielson equation,

$$\log\left(\frac{E'}{3}\right) = 7.0 + 293\left(\frac{\rho}{M_c}\right) \quad (5)$$

where E' (dynes cm^{-2}) is the storage modulus in a rubbery plateau region, ρ (g cm^{-3}) is the density of the material at room temperature and M_c (g mol^{-1}) is the molecular weight between crosslink points [4,27,28]. From the results, addition of CNSL content from 0 to 30 wt% provided a maximum in the crosslink density of BA-a/CNSL alloys i.e. 3383 mol m^{-3} (BA-a), 4517 mol m^{-3} (BA-a/CNSL 90/10), 4357 mol m^{-3} (BA-a/CNSL 80/20), and 3471 mol m^{-3} (BA-a/CNSL 70/30). This behavior also implied that only a certain content of CNSL i.e. ~10–20 wt%, yielded highly crosslinked net-

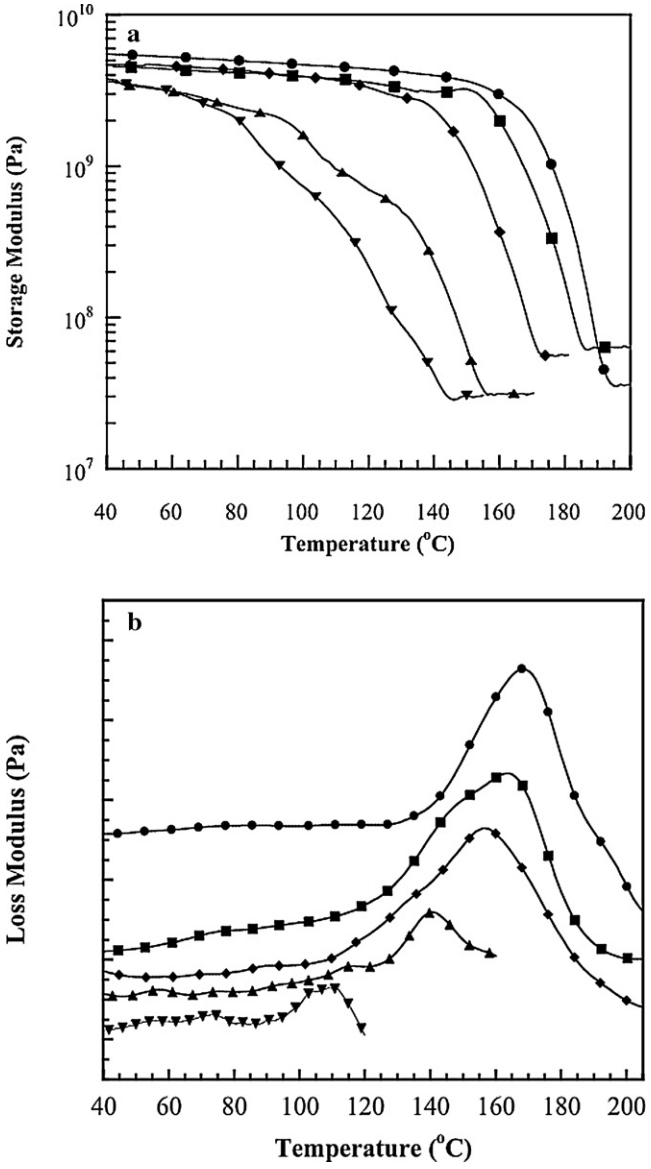

Fig. 5. (a) Storage modulus of BA-a/CNSL alloys obtained from fully cured condition at various CNSL compositions: (●) BA-a/CNSL 100/0, (■) BA-a/CNSL 90/10, (♦) BA-a/CNSL 80/20, (▲) BA-a/CNSL 70/30 and (▼) BA-a/CNSL 60/40. (b) Loss modulus of BA-a/CNSL alloys obtained from fully cured condition at various CNSL compositions: (●) BA-a/CNSL 100/0, (■) BA-a/CNSL 90/10, (♦) BA-a/CNSL 80/20, (▲) BA-a/CNSL 70/30 and (▼) BA-a/CNSL 60/40.

Table 2
Swelling and solvent extraction properties of BA-a/CNSL alloys.

Composition (BA-a/CNSL)	% Swelling	% Solvent extraction
100/0	1.78	0.95
90/10	0.96	0.10
80/20	2.87	0.30
70/30	6.63	1.01
60/40	15.4	10.6

work structure due to the possibly network formation between benzoxazine resin and anacardic acid in CNSL. This optimal content is similar to the optimal amount of phenolic novolac resin in the same type of polybenzoxazine [31] or the optimal content of epoxy resin in the polybenzoxazine [3].

Glass transition temperatures (T_g) of fully cured BA-a/CNSL polymer alloys were obtained from Fig. 5(b). The T_gs of the crosslink materials were determined from the maximum of the loss modulus (E'') of the figure. From a practical point of view, the maximum E'' is the most appropriate value. It corresponds to the initial drop from the glassy state into the rubbery state. The T_g of BA-a and BA-a/CNSL alloys was found to decrease when the CNSL content increased with the values ranging from 168 °C in BA-a to 110 °C in 60/40 BA-a/CNSL. This is probably due to the fact that the T_g of typical cashew nut shell liquid oil cured with cobalt naphthenate is reported to be about 60 °C [29] whereas the neat polybenzoxazine possesses a higher T_g of 165 °C. Consequently, the T_gs of the alloy systems became lower as the CNSL content increased. Moreover, the decreasing T_gs of BA-a/CNSL alloys may be due to the aliphatic nature of CNSL thus it can act as a plasticizer especially when the excess amount of CNSL presents in the polybenzoxazine. The decrease in the T_g of polybenzoxazine was also observed when benzoxazine resin was alloyed with phenolic novolac and novel glycidyl phosphine oxide [29,30].

3.7. Investigation of network formation ability of BA-a/CNSL alloys

The network formation ability of the BA-a/CNSL matrices at different composition of CNSL was assessed by solvent extraction method. In the test, the alloy specimens were immersed in chloroform for 15 days. After the immersion, it was observed that BA-a, 70/30 BA-a/CNSL and 60/40 BA-a/CNSL showed a deep color change of solvent due to a release of significant amount of extractives from each specimen. In addition, when the amount of CNSL in the polymer alloys was 30 wt% or greater, specimen disintegration from the solvent extraction test was observed. Beyond 30 wt% of CNSL, it was expected that excessive amount of CNSL might cause the formation of discontinuous network or network clusters. On the other hand, 80/20 BA-a/CNSL specimen exhibited slight color change and 90/10 BA-a/CNSL specimen showed almost no color change of the solvent. The percentages of swelling and solvent extraction are summarized in Table 2. It is clear that the optimum of CNSL i.e. 10 wt%, provided a near-zero solvent extraction value with the lowest degree of swelling. These results also suggested that the optimal content of CNSL of 10 wt% can contribute to a more perfect network formation of BA-a polymer. The solvent extraction results were also consistent with the crosslink density results of these alloys.

3.8. Characterization of BA-a/CNSL composites reinforced with bamboo fiber

The storage moduli as a function of temperature of the 65 wt% of bamboo fiber filled BA-a/CNSL alloys are plotted in Fig. 6(a). From the plot, the storage moduli at room temperature of the composites were observed to be in a range 3.7–6.3 GPa. It is clearly seen that all of the BA-a/CNSL alloys reinforced with 65 wt% bamboo fiber had significantly higher storage modulus values than those of unfilled BA-a/CNSL alloys. This is due to the reinforcing effect of bamboo fiber on the BA-a/CNSL matrices implying the substantial interfacial bonding between the alloy matrix and the bamboo fiber. From our previous reports, the presence of the phenolic structure in lignin fraction of woodflour and the abundance of hydroxyl moieties in the filler is believed to provide a composite system with strong interfacial bonding to the polybenzoxazine [32,33].

Fig. 6(b) exhibits a plot of the loss modulus of BA-a/CNSL filled with 65 wt% of bamboo fiber. As previously mentioned, the peak position of the loss modulus was used to determine T_g of each sample. It was evident that the T_g of the wood composites increased with an increase in polybenzoxazine fraction in the BA-a/CNSL alloys similar to the unfilled systems. The T_gs of BA-a, 90/10 BA-a/CNSL, 80/20 BA-a/CNSL, 70/30 BA-a/CNSL and 60/40 BA-a/CNSL composites were determined to be 181, 178, 168, 133 and 113 °C, respectively. The values were also higher than those of the unfilled

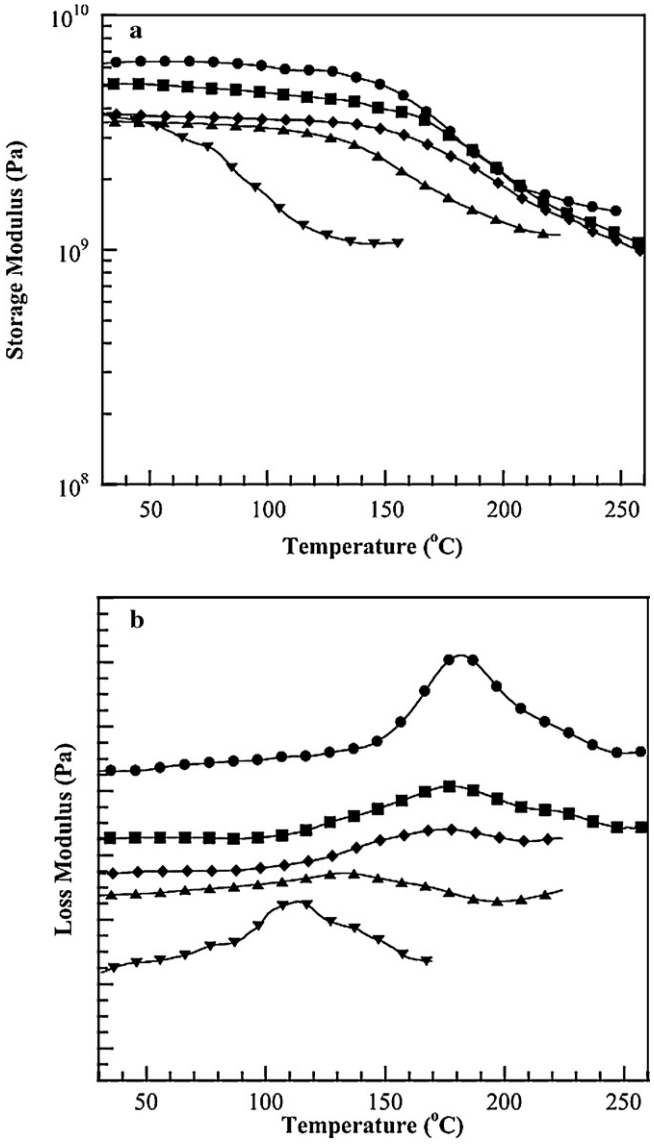

Fig. 6. (a) Storage modulus of BA-a/CNSL reinforced with bamboo at various CNSL compositions: (●) BA-a/CNSL 100/0, (■) BA-a/CNSL 90/10, (♦) BA-a/CNSL 80/20, (▲) BA-a/CNSL 70/30 and (▼) BA-a/CNSL 60/40. (b) Loss modulus of BA-a/CNSL reinforced with bamboo at various CNSL compositions: (●) BA-a/CNSL 100/0, (■) BA-a/CNSL 90/10, (♦) BA-a/CNSL 80/20, (▲) BA-a/CNSL 70/30 and (▼) BA-a/CNSL 60/40.

matrices suggesting significant interfacial bonding between the bamboo fiber and the polymer alloys.

3.9. Flexural properties of bamboo fiber composites based on BA-a/CNSL matrices

Flexural properties of bamboo fiber filled BA-a/CNSL alloys are depicted in Fig. 7(a). The average flexural modulus of our bamboo fiber composites was ranging from 3.9 to 6 GPa. The flexural modulus as a function of CNSL content showed a behavior nearly identical to that of the storage modulus determined by DMA i.e. the flexural modulus trended to decrease when the amount of CNSL increased. From Table 3, the flexural modulus of the bamboo-filled BA-a/CNSL alloys was significantly higher than those of reported wood plastic composites e.g. 50–70 wt% commercial wood particles reinforced HDPE (2.7–3.1 GPa) [34], 40 wt% bamboo fiber reinforced HDPE (3.1 GPa) [35] and 39 wt% bamboo fiber reinforced unsaturated polyester (3.6 GPa) [36]. Fig. 7(a) also exhibits flexural strength of the bamboo composites to be ranging from 54 to 66 MPa. The flexural strength of the composites was found to slightly decrease when the amount of CNSL increased. However, the bamboo filled BA-a/CNSL showed flexural strength higher than those major wood plastic composite products listed in Table 3.

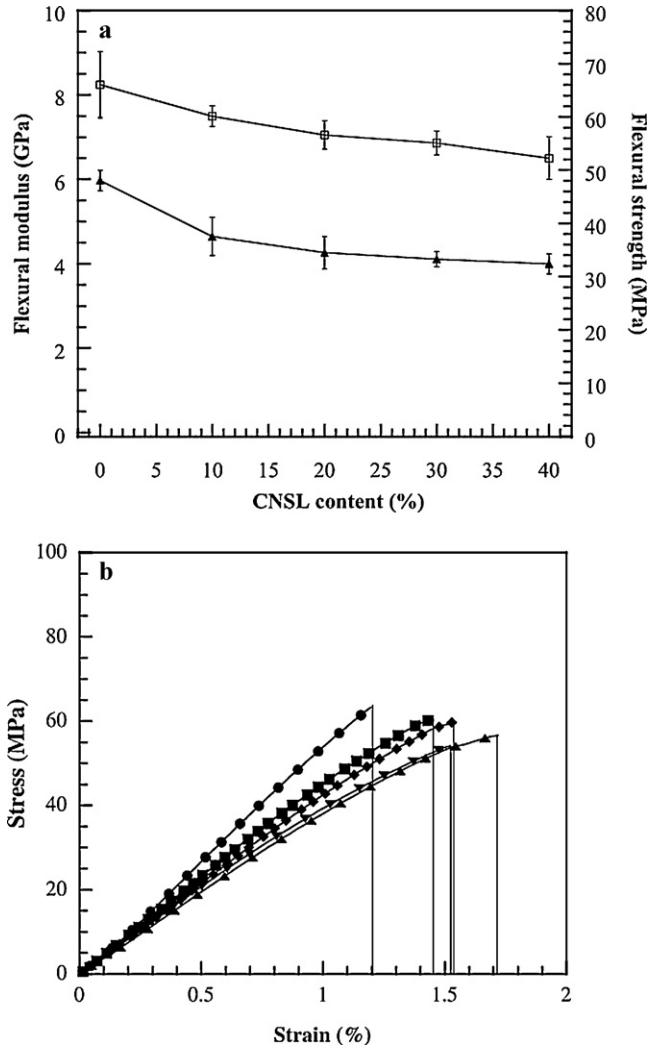

Fig. 7. (a) Effect of CNSL content on mechanical properties of bamboo composite: flexural modulus (▲) and flexural strength (□). (b) Flexural stress and strain relationship of bamboo-reinforced BA-a/CNSL reinforced with bamboo fiber at various CNSL compositions: (●) BA-a/CNSL 100/0, (■) BA-a/CNSL 90/10, (♦) BA-a/CNSL 80/20, (▲) BA-a/CNSL 70/30 and (▼) BA-a/CNSL 60/40.

Table 3
Flexural modulus and flexural strength of various natural fiber-reinforced composites.

Composite type	Mass fraction of fiber (wt%)	Flexural modulus (GPa)	Flexural strength (MPa)
Commercial wood flake reinforced HDPE	50–70	2.7–3.1	18–31
Bamboo fiber reinforced HDPE	40	3.1	21
Bamboo fiber reinforced unsaturated polyester	39	3.6	–

Fig. 7(b) illustrates flexural stress and strain curves of bamboo reinforced BA-a/CNSL matrices. From the figure, flexural strains at break of the composites were 1.20% BA-a, 1.45% BA-a/CNSL (90/10), 1.55% BA-a/CNSL (80/20), 1.71% BA-a/CNSL (70/30) and 1.52% BA-a/CNSL (60/40). The improved strain behavior may be caused by the addition of the more flexible CNSL fraction to the polybenzoxazine matrix. Additionally, the area under the flexural stress–strain curve refers to the energy absorption capability of the alloy materials which indicated the toughness of materials. The area under the curve tended to increase slightly with the amount of CNSL in the alloys i.e. 37 MPa at BA-a/CNSL (100/0), 40 MPa BA-a/CNSL (90/10), 42 MPa BA-a/CNSL (80/20), 43 MPa BA-a/CNSL (70/30), and 38 MPa BA-a/CNSL (60/40). The slight decrease of the toughness when CNSL content was greater than 30 wt% was likely from the discontinuous or imperfect network formed from the presence of excess amount of CNSL in the polybenzoxazine as discussed in the solvent extraction experiment.

4. Conclusions

An addition of cashew nut shell liquid oil in benzoxazine resin can substantially reduce the liquefying temperature, gel time, curing temperature and activation energy of the benzoxazine resin. A benzoxazine resin alloyed with cashew nut shell liquid oil was developed as highly processable matrices for wood composite products. The bamboo fiber content as high as 65% by weight was able to be incorporated into the obtained matrices due to the relatively low melt viscosity of the BA-a/CNSL mixtures. The obtained bamboo fiber-reinforced composites exhibited good compatibility between the fiber and the matrices thus attributed to enhancement on glass transition temperature and mechanical integrity of the samples.

Acknowledgements

This research receives financial support from Dutsadi Phiphat Scholarship of Chulalongkorn University. Additional supports are from the Thailand Research Fund (S. Rimdusit), the National Research University Project of the Ministry of Education, Thailand (AM1076A and AM006B), and 100th Anniversary of Chulalongkorn University Academic Funding. Material supplied by Thai Polycarbonate Co., Ltd. (TPCC), Forest Products Division, Royal Forest Department, Thailand and Maboonkrong Sirichai 25 Ltd., are greatly appreciated.

References

[1] H. Ishida, Y. Rodriguez, J. Appl. Polym. Sci. 58 (1995) 1751–1760.
[2] X. Ning, H. Ishida, J. Polym. Sci. A: Polym. Chem. 32 (1996) 1121–1129.
[3] H. Ishida, D.J. Allen, Polymer 37 (1996) 4487–4495.
[4] H. Ishida, Y.H. Lee, Polymer 42 (2001) 6971–6979.
[5] B. Lochab, I.K. Verma, J. Bijwe, J. Therm, Anal. Calorim 102 (2010) 769–774.
[6] E.T.N. Bisanda, M.P. Ansell, J. Mater. Sci. 27 (1992) 1690–1700.
[7] P. Peungjitton, P. Sangvanich, S. Pornpakakul, A. Petsom, S. Roengsumran, J. Surfact. Det. 12 (2009) 85–89.

[8] E. Papadopoulou, K. Chrissafis, Thermochim. Acta 512 (2011) 105–109.
[9] H. Ishida, US Patent 5,543,516, 1996.
[10] N.N. Ghosh, B. Kiskan, Y. Yagci, Prog. Polym. Sci. 32 (2007) 1344–1391.
[11] C. Jubsilp, T. Takeichi, S. Rimdusit, J. Appl. Polym. Sci. 104 (2007) 2928–2938.
[12] H.H. Winter, F. Chanbon, J. Rheol. 30 (1986) 367–382.
[13] H. Ishida, D.J. Allen, J. Appl. Polym. Sci. 79 (2001) 406–417.
[14] T. Agag, H. Tsuchiya, T. Takeichi, Polymer 45 (2004) 7903–7910.
[15] T. Takeichi, R. Zeidam, T. Agag, Polymer 43 (2002) 45–53.
[16] T. Takeichi, Y. Guo, S. Rimdusit, Polymer 46 (2005) 4909–4916.
[17] J.A. Youngquist, Wood-based Composites and Panel Products, Wood Hand Book, U.S. Department of Agriculture Government Printing Office, Madison, WI, 1999.
[18] M.V. Alonso, M. Oliet, J.M. Perez, F. Rodriguez, J. Echeverria, Thermochim. Acta 419 (2004) 161–167.
[19] C. Jubsilp, S. Damrongsakkul, T. Takeichi, S. Rimdusit, Thermochim. Acta 447 (2006) 131–140.
[20] D.R. Yei, H.K. Fu, W.Y. Chen, F.C. Chang, J. Polym. Sci. B: Polym. Phys. 44 (2006) 347–358.
[21] F.G. Souza, J.C. Pinto, G.E. de Oliveira, B.G. Soares, Polym. Test. 26 (2007) 720–728.
[22] L.Y. Mwaikambo, M.P. Ansell, J. Mater. Sci. 36 (2001) 3693–3698.
[23] R. Chelikani, Y.H. Kim, D.Y. Yoon, D.S. Kim, Appl. Biochem. Biotechnol. 157 (2009) 263–277.
[24] J. Dunkers, H. Ishida, J. Polym. Sci. A: Polym. Chem. 37 (1999) 1913–1921.
[25] M. Das, D. Chakraborty, J. Reinf. Plast. Compos. 28 (2009) 1339–1348.
[26] A.L. Pothan, Z. Oomen, S. Thomas, Compos. Sci. Technol. 63 (2003) 283–293.
[27] H. Ishida, D.P. Sanders, J. Polym. Sci. B: Polym. Phys. 38 (2000) 3289–3301.
[28] D.C.C. Lam, A.C.M. Chong, Mater. Sci. Eng. A 281 (2000) 156–161.
[29] R. Ikeda, H. Tanka, H. Uyama, S. Kobayashi, Polymer 43 (2002) 3475–3481.
[30] M.A. Espinosa, M. Galia, V. Cadiz, Polymer 45 (2004) 6103–6109.
[31] S. Rimdusit, N. Kampangsaeree, W. Tanthapanichakoon, T. Takeichi, N. Suppakarn, Polym. Eng. Sci. 45 (2007) 140–149.
[32] S. Rimdusit, W. Tanthapanichakoon, C. Jubsilp, J. Appl. Polym. Sci. 99 (2006) 1240–1253.
[33] C. Jubsilp, T. Takeichi, S. Hiziroglu, S. Rimdusit, Bioresour. Technol. 99 (2008) 8880–8886.
[34] P.W. Balasuriya, L. Ye, Y.W. Mai, Compos. Part A 32 (2001) 619–629.
[35] H. Liu, Q. Wu, G. Han, F. Yao, Y. Kojima, S. Suzuki, Compos. Part A 39 (2008) 1891–1900.
[36] K.M.M. Rao, K.M. Rao, A.V.R. Prasad, Mater. Des. 31 (2010) 508–513.